Use of Sensitivity Analysis to Compare Chemical Mechanisms for Air-Quality Modeling

ARTICLE *in* ENVIRONMENTAL SCIENCE AND TECHNOLOGY · JULY 2002

Impact Factor: 5.33 · DOI: 10.1021/es50002a606

Environ. Sci. Technol. 1992, 26, 1179–1189

Use of Sensitivity Analysis To Compare Chemical Mechanisms for Air-Quality Modeling

Jana B. Milford,* Dongfen Gao, Armistead G. Russell,† and Gregory J. McRae‡

Department of Civil Engineering, University of Connecticut, Storrs, Connecticut 06269

■ The LCC and CB4 mechanisms have been compared through a detailed sensitivity analysis. The formal method used provides an efficient means of comparing the influence of initial concentrations and reaction rate constants across mechanisms. The analysis identified discrepancies between the CB4 and LCC mechanisms that were overlooked in less formal tests. For the conditions studied, which approximate those of a smog chamber, the mechanisms generally show close agreement in predicted ozone concentrations, with larger differences for hydrogen peroxide and formaldehyde. The mechanisms differ in the sensitivity of peak O_3, H_2O_2, and HCHO concentrations to the initial concentrations of key classes of organic compounds. These differences have important implications for use of the mechanisms in developing reactivity scales. Revisions to the CB4 mechanism that have been recommended based on recent studies of peroxy acetyl radical + NO and NO_2 reaction rates are shown to be significant.

1. Introduction

Over the past decade, rapid progress has been made in understanding the gas-phase chemical reactions that produce ozone and other secondary pollutants in urban atmospheres. Several "condensed" chemical mechanisms are currently in use to represent the most important of these reactions in a form tractable for mathematical air-quality modeling. The existence of alternative reaction schemes raises questions for those who use photochemical air-quality models: which mechanism ought to be used to estimate emissions reduction requirements, and what difference will it make if one is selected versus another? To answer these questions, mechanisms are tested against smog chamber experiments, and the results of simulations performed with alternative mechanisms are compared in detail.

Typically, mechanisms are analyzed and compared on the basis of predicted concentrations of key species. However, including sensitivity analysis as one component of a comparison can be extremely useful in helping to determine the significance of uncertainties or apparent differences between two mechanisms. Previous mechanism comparison studies have employed sensitivity analysis only informally, by repeating otherwise identical simulations with a change in the value of a selected parameter, such as a reaction rate constant or initial concentration (*1–4*).

This article demonstrates the application of a formal sensitivity analysis method, the direct decoupled method (DDM) (*5*, *6*), to the task of comparing chemical mechanisms. The sensitivity coefficients calculated with the DDM are the partial derivatives of the model output concentrations with respect to the input parameters, including initial concentrations as well as reaction rate constants. Because the direct decoupled method calculates sensitivity coefficients for all species and rate parameters simultaneously, a single DDM application can replace hundreds of simulations performed in conducting an informal sensitivity analysis. Previous applications of formal sensitivity analysis to gas-phase chemical mechanisms focused on understanding various aspects of a single mechanism (*7*, *8*). The utility of formal sensitivity analysis for comparing mechanisms has not previously been illustrated.

A second problem of current interest to which the direct decoupled method is well-suited is the question of ranking organic compounds by their relative contributions to the formation of ozone or other secondary pollutants. Regulations are currently being developed that will use reactivity weighting in determining allowable emissions (*9*). A standard approach used to estimate organic compound reactivities in the past has been to look at how ozone concentrations change when computer simulations or smog chamber experiments are repeated, with small changes made in the initial concentration (and/or the simulated emissions rate) of the compound under investigation (*10–12*). In contrast, the sensitivities calculated with the DDM are numerically exact local sensitivities, as opposed to approximations based on two separate runs, each with possible numerical inaccuracies. Furthermore, with a single simulation the reactivities of all of the input compounds are given by the sensitivity coefficients calculated with the direct decoupled method. The application of the direct decoupled method to the problem of calculating reactivities is also demonstrated in this study.

The mechanisms to which the DDM is applied here are the CB4 mechanism (*13*, *14*) and the LCC mechanism (*15*). Both are actively used in research and regulatory applications. In addition to the published version of CB4, a version with recently recommended modifications (*16*, *17*) is included in this study. Dodge (*4*, *18*) has previously compared the LCC mechanism with the 1988 version of CB4. Her comparisons were made by examining the outputs of numerous simulations covering a variety of conditions. Dodge's studies thus provide a useful basis for comparison with the formal sensitivity analysis approach adopted here.

The reader is referred to Dunker (*5*) for a detailed description of the direct decoupled method. The next section of this paper introduces the CB4 and LCC mechanisms and reviews the results of previous studies that have compared them. The simulation conditions used for the study are presented in Section 3. Section 4 presents the results of the sensitivity analysis, exploring the differences between the CB4 and LCC mechanisms and demonstrating the utility of the DDM. Section 5 compares the sensitivity coefficients calculated for this study with the "incremental reactivities" of Carter and Atkinson (*12*) and compares the results of the DDM-based comparison of CB4 and LCC with Dodge's (*4*, *18*) findings. The conclusions of the study are given in Section 6.

2. Description of the CB4 and LCC Mechanisms

Listings of the CB4 and LCC mechanisms as they were implemented for this analysis are available from the authors. Table I summarizes the number of reactions and

†Department of Mechanical Engineering, Carnegie Mellon University, Pittsburgh, PA 15213.
‡Department of Chemical Engineering, Carnegie Mellon University, Pittsburgh, PA 15213.

0013-936X/92/0926-1179$03.00/0

Table I. Summary Characteristics of the CB4 and LCC Mechanisms

	mechanism	
	CB4	LCC
total species	33	50
primary ROG species	8	12
organic radicals	6	11
no. of reactions	81	131
photolysis reactions	11	17
references	13, 14	15
evaluation studies	13	19

Table II. Modifications Recommended for CB4 (*16*, *17*) and Incorporated into CB4.1

reaction 82 has been added

$XO_2 + HO_2 \rightarrow$ (no products) (82)

$k_{82} = 113.4 \exp(1300/T)$ (ppm^{-1} min^{-1})

rates for the following CB4 reactions have been changed

$C_2O_3 + NO \rightarrow HCHO + NO_2 + HO_2 + XO_2$ (46)

$C_2O_3 + NO_2 \rightarrow PAN$ (47)

$PAN \rightarrow C_2O_3$ (48)

CB4

$k_{46} = 7.915 \times 10^3 \exp(250/T)$ (ppm^{-1} min^{-1})

$k_{47} = 1.18 \times 10^{-4} \exp(5500/T)$ (ppm^{-1} min^{-1})

$k_{48} = 5.616 \times 10^{18} \exp(-14000/T)$ (min^{-1})

CB4.1

$k_{46} = 5.15 \times 10^4 \exp(-180/T)$ (ppm^{-1} min^{-1})

$k_{47} = 3.84 \times 10^3 \exp(380/T)$ (ppm^{-1} min^{-1})

$k_{48} = 1.2 \times 10^{18} \exp(-13500/T)$ (min^{-1})

species in each mechanism and gives references to their documentation and experimental evaluations (*13–15*, *19*). Mechanism development is an ongoing process, and modifications have been recommended for CB4 since it was published (*16*, *17*). Accordingly, an updated version of CB4 that incorporates these modifications is also examined in this study. Hereafter, the modified version of CB4 will be referred to as CB4.1 and the published version as CB4. The modifications incorporated into CB4.1 are listed in Table II.

In order to develop computationally tractable mechanisms, highly condensed representations of the complex organic chemistry that occurs in polluted atmospheres are required. In the past, differences introduced in selecting and approximating organic reactions have led to substantial discrepancies in predicted product concentrations (*1–3*, *20*, *21*). In contrast to the reactions of the organics, among recently developed mechanisms there have been few differences in the inorganic reactions of primary importance under urban conditions. Key aspects of the treatment of organics in the CB4 and LCC mechanisms are described below.

Classes of organics in the CB4 mechanism are based on functional groups and include paraffinic and olefinic bonds, ethylene, isoprene, two aldehydes, and two aromatic classes. Key organic peroxy radicals include an acetyl peroxy radical and a generalized alkyl peroxy radical that produces NO_2 upon reaction with NO. The other stable products produced from alkyl peroxy radical + NO reactions are included as products of the ROG oxidation reactions that would have produced distinct radicals in the first place. Acetyl peroxy radicals in CB4 react with NO, NO_2, other acetyl peroxy radicals, and HO_2. Alkyl peroxy radicals in the published version of CB4 react with other alkyl peroxy radicals in addition to reacting with NO, but not with acetyl peroxy radicals or HO_2. As noted in Table II, a reaction between alkyl peroxy radicals and HO_2 has been included in CB4.1.

In the LCC mechanism, groups of stable organic species with similar reaction rates and products are represented by surrogate species for which rate expressions and product yields have been preset based on an assumed mixture. Four primary carbonyl classes, two alkane classes, ethylene, two classes of higher alkenes, and three aromatics classes are included. The chemistry of the radical products of organic oxidation reactions has been condensed using a treatment similar to that used in the CB4 mechanism. However, a larger number of generalized radicals are used, each of which yields different products upon reaction with NO. In further contrast to CB4, in the LCC mechanism both alkyl and acetyl peroxy radicals react with each other as well as with other alkyl and acetyl peroxy radicals and with HO_2.

A thorough comparison of the LCC and CB4 mechanisms has been conducted by Dodge (*4*, *18*). In these studies, differences between LCC and CB4 in aromatics chemistry, temperature dependence of PAN formation, and termination reactions for peroxy radicals were noted as particularly significant. Differences in the absorption cross sections used to calculate formaldehyde photolysis rates for the two mechanisms also produced significant differences in predicted concentrations of formaldehyde and hydrogen peroxide (*18*). For the present study, as discussed below, the formaldehyde photolysis rates given for LCC were adopted for CB4.

For ozone, as well as H_2O_2 and PAN, comparisons of the predictions of different mechanisms and tests against smog chamber experiments have indicated that uncertainty about aromatic chemistry is a critical source of discrepancies among current mechanisms. Several recent studies have singled out uncertainties in aromatics mechanisms, including product yields and rate constants for secondary reactions, as having a significant impact on calculated ozone formation rates and maximum concentrations (*3*, *4*, *18*, *22–24*).

The published version of CB4 includes a large, negative activation energy for the PAN formation reaction (*13*, *14*)

$$CH_3CO_3 + NO_2 \rightarrow PAN$$

$$k = 1.2 \times 10^{-4} \exp(5500/T) \text{ ppm}^{-1} \text{ min}^{-1}$$

compared to the reaction rate expression used in LCC (*15*)

$$k = 4.1 \times 10^3 \exp(180/T) \text{ ppm}^{-1} \text{ min}^{-1}$$

At low temperatures, this discrepancy leads to low ozone production with CB4 (*4*). As noted in Table II, the temperature dependence of reactions associated with PAN formation and decomposition have been altered in deriving CB4.1 from CB4. The new rate expressions used in CB4.1 are based on recent studies of the kinetics of PAN decomposition (*25*, *26*) and of the relative rates of the reactions of acetyl peroxy radicals with NO versus NO_2 (*26*, *27*).

Finally, as described above, CB4 and LCC differ in their treatment of termination reactions for peroxy radicals. Dodge (*4*) showed that adding the reaction of alkyl peroxy radicals with HO_2 reduced the peak H_2O_2 concentrations predicted with CB4, bringing about better agreement with LCC. In addition, differences in formaldehyde concentrations in simulations conducted with high ROG to NO_x ratios and with acetaldehyde or alkenes as the only input organics were attributed to differences in the acetyl peroxy radical termination reactions included in LCC versus CB4.

3. *Simulation Conditions*

The ROG composition used in this study is listed in Tables III and IV. Intended to represent a typical morning composition for an urban area, the mixture listed in Table III is based on morning compositions reported by Grosjean and Fung (*28*) and Baugues (*29*). Grosjean

Table III. Initial Reactive Organic Gas Composition (ppmv/ppm C)[a] Used in the Sensitivity Studies[b]

ethane	0.019	propene	0.013
propane	0.012	*trans*-2-butene	0.011
butane	0.037	benzene	0.0061
pentane	0.019	toluene	0.014
hexane	0.010	xylene	0.015
heptane	0.010	formaldehyde	0.030
octane	0.010	acetaldehyde	0.014
acetylene	0.019	propionaldehyde	0.010
ethylene	0.014		

[a] Concentration of the given compound (ppmv)/total concentration of organic compounds (ppm C). [b] Composition derived from the data of Grosjean and Fung (*28*) and Baugues (*29*).

Table IV. Initial Reactive Organic Gas Composition (ppmv/ppm C) As Implemented for the LCC and CB4 Mechanisms[a,b]

CB4		LCC	
PAR (1)	0.50	ALK4 (4.1)	0.063
		ALK7 (7)	0.030
ETH (2)	0.014	ETHE (2)	0.014
OLE (2)	0.013	PRPE (3)	0.013
		TBUT (4)	0.011
TOL (7)	0.014	TOLU (7)	0.014
XYL (8)	0.015	XYLE (8)	0.015
FORM (1)	0.030	HCHO (1)	0.030
ALD2 (2)	0.046	ALD2 (2)	0.014
		RCHO (3)	0.010
NR[c] (1)	0.098	NR (2.5)	0.048

[a] The species names correspond to those used in the original mechanisms. [b] The number of carbon atoms per molecule is given in parentheses for each species. [c] NR, nonreactive.

and Fung reported the average of measurements made over 23 days during the fall of 1981 at a downtown Los Angeles location. Baugues reported median morning compositions for the 1984 and 1985 summer seasons in approximately 20 cities. Table IV shows the splitting factors derived for the LCC and CB4 mechanisms, following the guidance provided by their developers.

Also reflecting typical urban conditions, an initial NO to NO_2 ratio of 3.0 and CO concentration of 1.5 ppm were used in all of the runs. Initial ROG and NO_x concentrations for the three cases analyzed were case A: ROG = 1.8 ppm C, NO_x = 0.15 ppm (ROG:NO_x = 12.1); case B: ROG = 0.9 ppm C, NO_x = 0.15 ppm (ROG:NO_x = 6:1); case C: ROG = 1.8 ppm C, NO_x = 0.075 ppm (ROG:NO_x = 24:1). No smog chamber-dependent reactions were included in the simulations. Constant conditions, including a constant temperature of 298 K, relative humidity of 50%, no dilution, and constant photolysis rates, were assumed in order to facilitate interpretation of the sensitivities to the rate parameters. The photolysis rates approximated average values over the daylight hours in midsummer at a latitude of 40° N. Table V gives the photolysis rates used in each mechanism. Photolysis rates used with the LCC mechanism are those recommended by Lurmann et al. (*15*). With CB4, the recommendations of Gery et al. (*13*) were adopted, except for formaldehyde and other associated compounds. Following Dodge (*18*), the formaldehyde photolysis rates used in LCC were also adopted here for CB4. Photolysis rates for H_2O_2, MGLY (methylglyoxal), and OPEN (an aromatic ring fragment) are specified in the CB4 documentation as ratios to the formaldehyde photolysis rates and were adjusted accordingly.

The sensitivity calculations in this study were performed using a direct decoupled method code developed by

Table V. Photolysis Rates Used in Each Mechanism

photolytic reaction	rxn no.	rate, min^{-1}
LCC Mechanism		
$NO_2 \rightarrow NO + O$	(1)	0.300
$NO_3 \rightarrow NO$	(13)	0.865
$NO_3 \rightarrow NO_2 + O$	(14)	0.775×10^{1}
$O_3 \rightarrow O$	(15)	0.196×10^{-1}
$O_3 \rightarrow OSD$	(16)	0.352×10^{-3}
$HONO \rightarrow NO + OH$	(20)	0.566×10^{-1}
$H_2O_2 \rightarrow 2OH$	(35)	0.182×10^{-3}
$ROOH \rightarrow HO_2 + OH$	(42)	0.182×10^{-3}
$HCHO \rightarrow 2HO_2 + CO$	(46)	0.677×10^{-3}
$HCHO \rightarrow CO$	(47)	0.133×10^{-2}
$ALD2 \rightarrow CO + HCHO + HO_2 + RO_2R + RO_2$	(52)	0.730×10^{-4}
$RCHO \rightarrow ALD2 + HO_2 + CO + RO_2R + RO_2$	(61)	0.210×10^{-3}
$ACET \rightarrow MCO_3 + HCHO + RCO_3 + RO_2R + RO_2$	(69)	0.202×10^{-4}
$MEK \rightarrow MCO_3 + ALD2 + RCO_3 + RO_2R + RO_2$	(71)	0.291×10^{-4}
$GLYX \rightarrow 0.13HCHO + 1.87CO$	(73)	0.271×10^{-2}
$MGLY \rightarrow MCO_3 + HO_2 + CO + RCO_3$	(82)	0.599×10^{-2}
$DIAL \rightarrow HO_2 + CO + MCO_3 + RCO_3$	(116)	0.155×10^{-1}
CB4 Mechanism		
$NO_2 \rightarrow NO + O$	(1)	0.300
$O_3 \rightarrow O$	(8)	0.159×10^{-1}
$O_3 \rightarrow O1D$	(9)	0.409×10^{-3}
$NO_3 \rightarrow 0.89NO_2 + 0.89O + 0.11NO$	(14)	0.102×10^{2}
$HONO \rightarrow NO + OH$	(23)	0.593×10^{-1}
$H_2O_2 \rightarrow 2OH$	(34)	0.338×10^{-3}
$FORM \rightarrow 2HO_2 + CO$	(38)	0.677×10^{-3}
$FORM \rightarrow CO$	(39)	0.133×10^{-2}
$ALD2 \rightarrow FORM + 2HO_2 + CO + XO_2$	(45)	0.976×10^{-4}
$OPEN \rightarrow C_2O_3 + HO_2 + CO$	(69)	0.612×10^{-2}
$MGLY \rightarrow C_2O_3 + HO_2 + CO$	(74)	0.653×10^{-2}

McCroskey and McRae (*6*), which utilizes Gear's method (*30*) to numerically integrate both the rate and sensitivity equations. An error tolerance of 10^{-7} was used for this work.

4. Sensitivity Analysis Results

This section begins by examining time series for key species predicted with the CB4, CB4.1, and LCC mechanisms and then examines sensitivity analysis results for each mechanism. The analysis focuses on O_3, HCHO, and H_2O_2. H_2O_2 is an important sink for peroxy radicals in ROG-rich systems and is the principal aqueous-phase oxidant of sulfur dioxide. Formaldehyde is an important source of radicals, as well as having potential health impacts.

Figure 1 presents O_3, NO, and NO_2 concentrations plotted over time for three combinations of initial ROG and NO_x concentrations. For case A (ROG:NO_x = 12:1), the predicted ozone concentrations after 12 h range from 0.336 with CB4 to 0.373 ppm with CB4.1. CB4.1 and LCC show close agreement. For case B (ROG:NO_x = 6:1), the predicted final ozone concentrations range from 0.111 to 0.132 ppm. The results for case C (ROG:NO_x = 24:1) range from 0.234 to 0.279 ppm ozone after 12 h. In cases B and C, ozone concentrations predicted with CB4.1 are intermediate to the relatively high prediction of LCC and the low prediction of CB4.

Figure 2 shows predicted concentrations of H_2O_2 and HCHO for the three cases. Larger discrepancies between the mechanisms occur for hydrogen peroxide and formaldehyde than for ozone. In case B (6:1) the final H_2O_2 concentration predicted with LCC exceeds that predicted with CB4 by more than a factor of 2, although the concentrations are very low. The reverse is true for case C

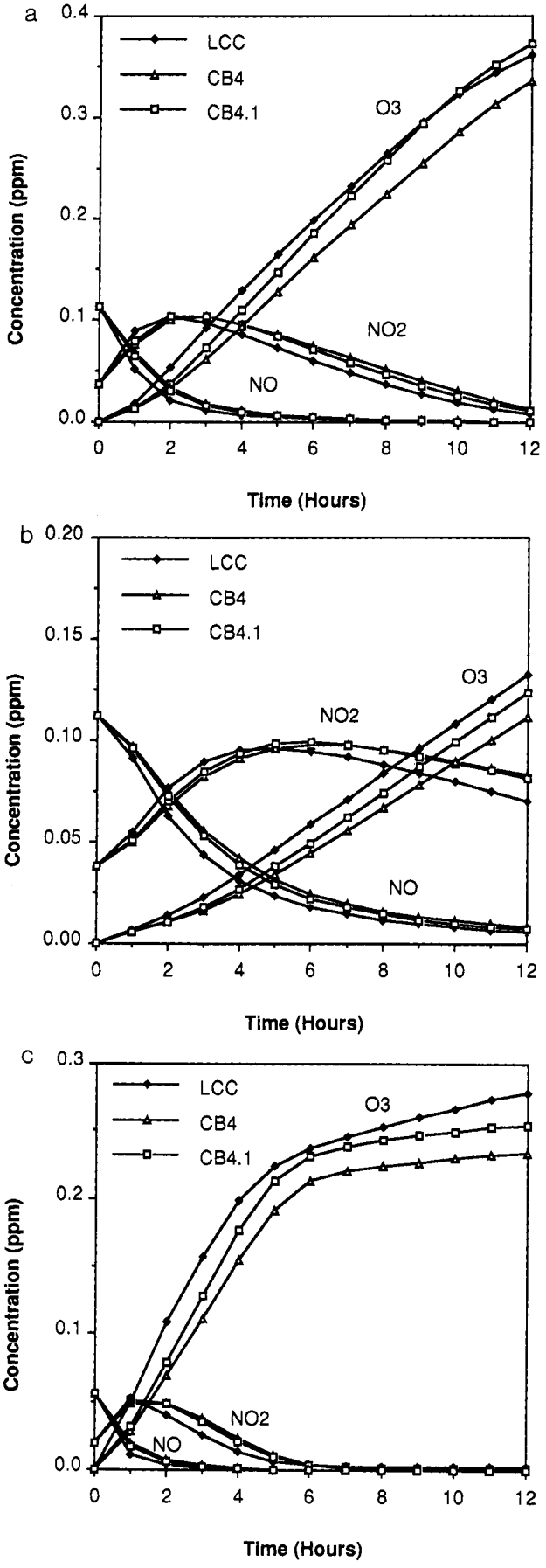

Figure 1. O_3, NO, and NO_2 concentrations predicted with LCC, CB4, and CB4.1 for (a) case A, with initial concentrations of 1.8 ppm C ROG and 0.15 ppm NO_x; (b) case B, with initial concentrations of 0.9 ppm C ROG and 0.15 ppm NO_x; and (c) case C, with initial concentrations of 1.8 ppm C ROG and 0.075 ppm NO_x.

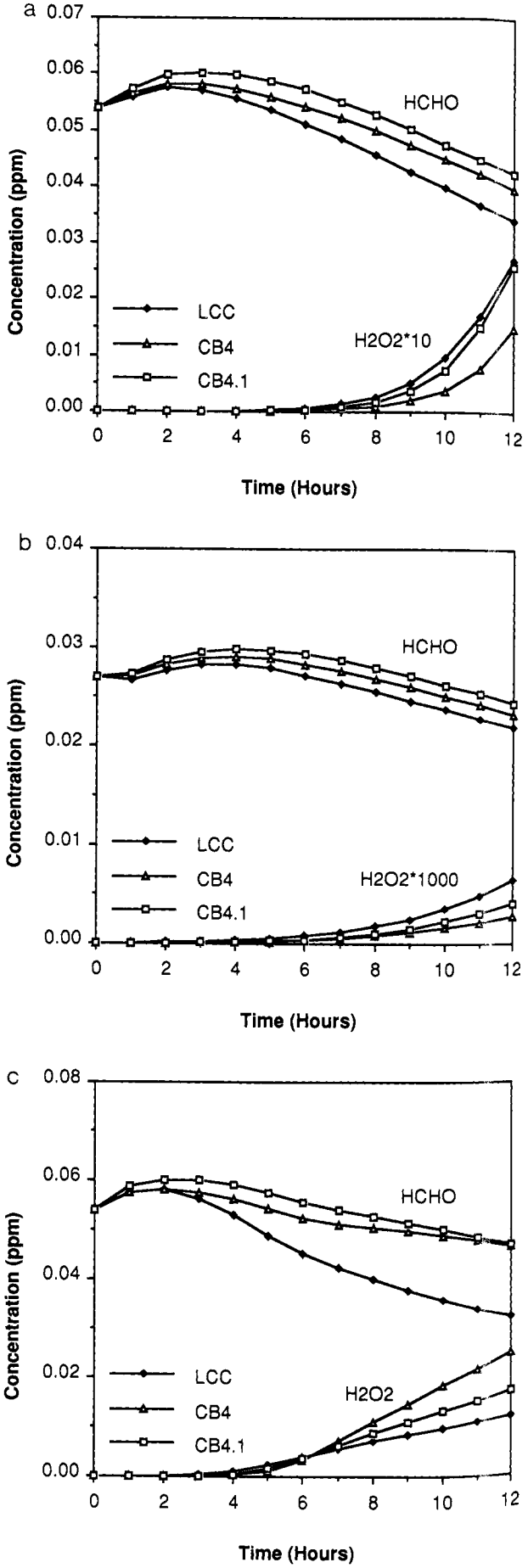

Figure 2. H_2O_2 and HCHO concentrations predicted with LCC, CB4, and CB4.1 for (a) case A (initial ROG:NO_x = 12:1); (b) case B (6:1); and (c) case C (24:1).

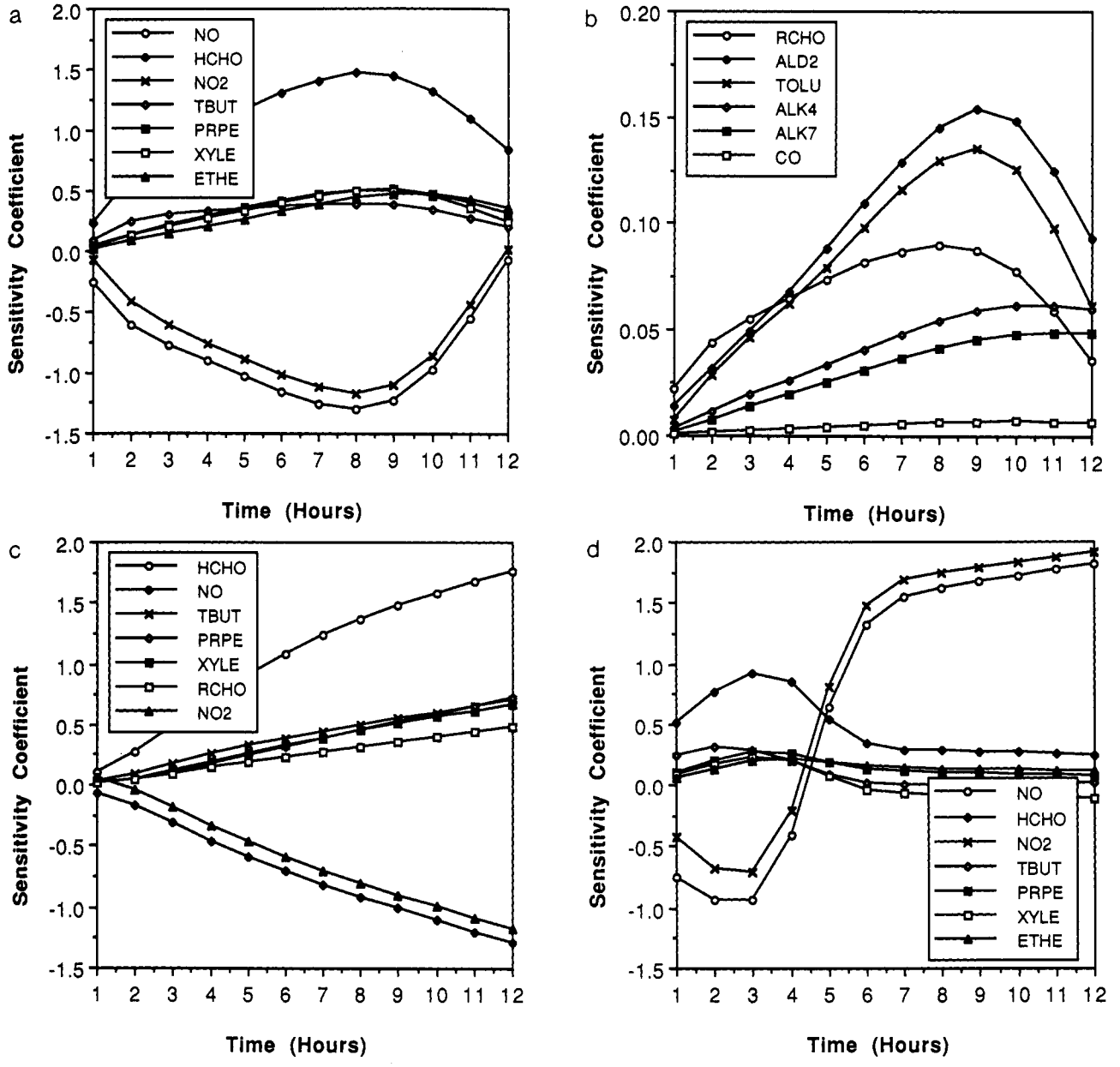

Figure 3. Sensitivity of ozone to initial NO_x and ROG concentrations predicted with the LCC mechanism for (a and b) case A (initial ROG:NO_x = 12:1); (c) case B (6:1); and (d) case C (24:1). The sensitivity coefficients are given in units of ppm O_3 per ppm NO_x or ppm O_3 per ppm C ROG. For cases B and C, coefficients are shown only for the five ROG classes to which ozone shows the greatest sensitivity.

(24:1) in which the H_2O_2 concentration predicted with CB4 is more than twice as high as that predicted with LCC. In all three cases CB4.1 gives intermediate H_2O_2 concentrations compared to CB4 and LCC. For HCHO, however, the concentrations predicted with CB4 fall between those of CB4.1 and LCC. Thus the modifications incorporated in CB4.1 increased the discrepancy in the formaldehyde predictions of the different mechanisms.

Table VI shows final concentrations of key species predicted in cases A–C. Relatively close agreement is apparent between CB4, CB4.1, and LCC for nitric acid and peroxyacetyl nitrate, especially in cases A and C. However, when PAN analogues represented in the LCC mechanism are considered, "total PAN" concentrations are distinctly higher with LCC than with CB4 and CB4.1.

In order to further explore the differences between the mechanisms, the direct decoupled method has been used to calculate the sensitivity of the predicted concentrations of key species to initial conditions and reaction rate constants. As an illustration, Figure 3 shows results for the sensitivity of ozone to the initial concentrations of NO, NO_2, and ROG species calculated for the LCC mechanism. Time-dependent sensitivity coefficients

$$s_{ij}(t) = \partial y_i(t)/\partial p_j$$

are shown, with p_j representing an element of the initial concentration vector $\mathbf{y}_0$. For the organic species, the units of p_j are ppm C, i.e., the sensitivity coefficients are given on a per-carbon basis. Although not shown, the sensitivity results for CB4 and CB4.1 are generally similar to those for LCC, with a few important differences discussed below.

For LCC, in cases A and B, the sensitivity of ozone to the initial NO and NO_2 concentrations is negative throughout the simulations. In contrast, after the first 4 h in case C, the sensitivity coefficients for NO and NO_2 are positive. The sensitivity of ozone to NO_x reflects the balance between NO_x and ROG (and hence peroxy radical production) in the system. This balance determines whether the result of adding NO_x is decreased levels of ozone and radicals as they are scavenged by NO and NO_2 or enhanced concentrations as more NO_2 is available to be photolyzed and more NO is available to cycle radicals.

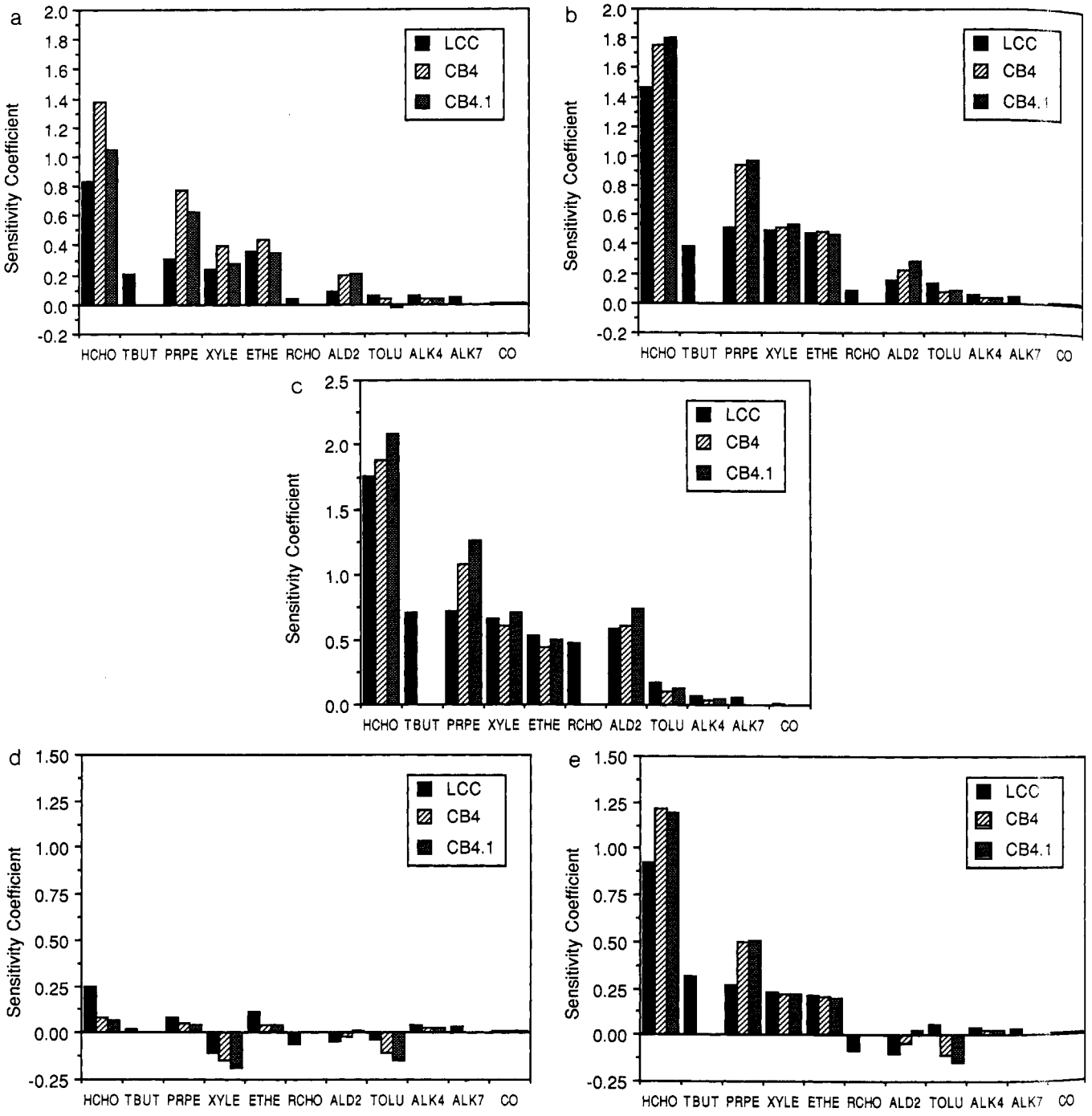

Figure 4. (a, c, and d) Sensitivity of peak ozone to initial concentrations and (b, c, and e) maximum sensitivity of ozone to the initial concentration for each ROG class. (a and b) Case A (initial ROG:NO_x = 12:1); (c) case B (6:1); (d and e) case C (24:1). For case B, the maximum sensitivities and sensitivities of peak ozone coincide, so only one graph (c) is shown. Sensitivity coefficients are given in units of ppm O_3 per ppm C. LCC classes were used for labeling the graph, so the CB4 and CB4.1 OLE class is shown as 'PRPE' and the PAR class as 'ALK4'.

The sensitivity of the O_3 concentration to the initial concentrations of the organic classes reflects both the demand for radicals in the system and the supply provided by each class. In cases A and B, the sensitivity of ozone to the initial concentrations of the ROG species remains positive throughout the simulation. However, in case C, with a 24:1 ratio of ROG to NO_x, sensitivity coefficients for the xylene and toluene (not shown) classes in LCC switch sign from positive to negative after about 5 h, and coefficients for the acetaldehyde and propionaldehyde (RCHO) classes are always negative (also not shown). Similar results occur with CB4 and CB4.1.

For purposes of comparing the mechanisms, Figure 4 presents instantaneous sensitivity coefficients for each of the organic classes in CB4, CB4.1, and LCC. The sensitivity coefficients depend strongly on time, so two sets of instantaneous coefficients are shown. The first set of coefficients (Figure 4, panels a, c, and d) are evaluated at the time at which the peak ozone concentration is produced, i.e., the end of the 12-h simulation period for each of the three cases included in this study. The instantaneous sensitivity coefficient at the time of the peak is equivalent to the "incremental reactivity" (IR) defined by Carter and Atkinson (*12*)

$$\mathrm{IR} = \lim_{\Delta \mathrm{HC}_j \to 0} \left[\frac{R(\mathrm{HC}_j + \Delta \mathrm{HC}_j) - R(\mathrm{HC}_j)}{\Delta \mathrm{HC}_j} \right] \quad (1)$$

Table VI. Predicted Concentrations (ppm) of Key Species after 12 h

species	mechanism	ROG/NO_x 12:1	6:1	24:1
O_3	LCC	0.361	0.132	0.279
	CB4	0.336	0.111	0.234
	CB4.1	0.373	0.124	0.255
HNO_3	LCC	0.0696	0.0578	0.0260
	CB4	0.0655	0.0452	0.0266
	CB4.1	0.0702	0.0483	0.0283
H_2O_2	LCC	0.00270	6.5×10^{-6}	0.0120
	CB4	0.00154	2.8×10^{-6}	0.0249
	CB4.1	0.00258	4.0×10^{-6}	0.0170
HCHO	LCC	0.0340	0.0219	0.0324
	CB4	0.0398	0.0232	0.0466
	CB4.1	0.0426	0.0244	0.0468
PAN	LCC	0.0456	0.0087	0.0278
	CB4	0.0489	0.0075	0.0279
	CB4.1	0.0450	0.0062	0.0253
PPN	LCC	0.0108	0.00177	0.00643
GPAN	LCC	0.173×10^{-3}	0.247×10^{-4}	0.870×10^{-4}
total PAN	LCC	0.0566	0.0105	0.0343

where $R(HC_j)$ is the maximum value of $[O_3]$ – [NO] calculated in a base case simulation and $R(HC_j + \Delta HC_j)$ is the maximum value of $[O_3]$ – [NO] calculated in a simulation with ΔHC_j added to the inputs from the base case. (Except in NO_x-rich cases, [NO] can be neglected at the time when $[O_3]$ – [NO] reaches its maximum value.) The second set of sensitivity coefficients in Figure 4 (panels b, c, and e) show the maximum sensitivity of ozone to the initial concentration of each organic, irrespective of the hour at which the maximum value occurs. [For example, referring back to Figure 3a and b, the maximum sensitivity of ozone to the initial formaldehyde concentration occurs at 8 h, whereas the maximum sensitivity to the higher alkanes class (ALK7) occurs at the end of the simulation.] In case B, all of the maximum sensitivities as well as the peak ozone concentrations occur at the end of the simulation, so the two sets of coefficients coincide (Figure 4c).

Figure 4 shows that formaldehyde is uniformly the most reactive of the organic classes per molecule of carbon. The alkenes and xylene generally follow. The sensitivity of ozone to compounds that react comparatively slowly, such as the alkanes, increases late in the simulations relative to the sensitivity to the more rapidly reacting compounds (see Figure 3a and b). Thus maximum reactivity values show more spread across compounds than do the reactivities at the time of the ozone peaks. In the high ROG:NO_x case, the xylene, toluene, acetaldehyde and propionaldehyde classes ultimately inhibit ozone formation. This means that a small reduction in the input concentration of one of these compounds would increase the final ozone concentration.

Of special interest is the degree of consistency in the sensitivity coefficients from one mechanism to another. One factor that influences this is the time at which the coefficients are evaluated. For example, for CB4 and CB4.1, the maximum sensitivity coefficients in case A suggest better agreement than the sensitivities at the time of the ozone peak. However, the times at which the maximum sensitivities occur are different; for formaldehyde, the aromatics, and the alkenes, the maximum sensitivity coefficients occur 1 h earlier with CB4.1 than with CB4. The uniformly higher sensitivity coefficients with CB4.1 than with CB4 in the low-ROG:NO_x case, and the higher and earlier maximum coefficients with CB4.1 than with CB4 in case A, indicate that CB4.1 is more reactive in terms of radical production. As ROG to NO_x ratios increase beyond about 10:1, the demand for radicals declines, accompanied by a trend toward lower sensitivity to input organic concentrations. The generally higher sensitivity coefficients with CB4 than CB4.1 in the 24:1 case reflect the overall higher rates of radical production in CB4.1, which results in less "demand" for radicals for ozone formation.

Comparing LCC with the carbon bond mechanisms, the reactivities of the alkanes classes in LCC are consistently higher than the reactivities of the PAR class in CB4 and CB4.1. To understand the source of this difference, the oxidation reactions of the products of the ALK4 + OH and PAR + OH reactions can be traced, and the peroxy radicals that would ultimately be produced in these reactions counted. Assuming the oxidation reactions go to completion, more peroxy radicals are produced per carbon with the ALK4 class in LCC than with PAR in CB4 and CB4.1.

The reactivity of the toluene class in LCC is also consistently high compared to the toluene class in CB4 and CB4.1. Dodge (*18*) previously found the same result in comparing LCC to CB4. She suggested that in CB4 the radical intermediate produced in the reaction of TOL + OH is assumed either to react with NO to produce NO_2 and a dicarbonyl or to rearrange, producing a cresol. The cresol species is significantly less reactive than the dicarbonyl species. In LCC, only the reaction with NO occurs.

In contrast to the cases of the alkanes and toluene, CB4 and CB4.1 generally display higher reactivity for the aldehydes and propene classes than LCC. As explained below, the difference is partly due to differences in reaction rates used for the acetyl peroxy radical + NO and NO_2 reactions in the three mechanisms. Another notable discrepancy between the mechanisms is seen in comparing the sensitivity coefficients for the *trans*-2-butene class in LCC and the acetaldehyde classes in CB4 and CB4.1, which represent *trans*-2-butene in those mechanisms. At high ROG to NO_x ratios, the maximum sensitivity to the LCC *trans*-2-butene class is much greater than the sensitivity to the CB4.1 acetaldehyde class, and for CB4, the maximum sensitivity in magnitude is negative in sign.

In the same manner as for ozone, the sensitivity of formaldehyde, hydrogen peroxide, and other secondary pollutants to input concentrations can be calculated and interpreted as reactivities. Figure 5 shows instantaneous sensitivity coefficients for formaldehyde, on a per molecule of carbon basis, for case A. Again, coefficients are shown for the time that the peak formaldehyde concentration occurs with each mechanism, i.e., at the end of the second hour for CB4 and LCC and at the end of the third hour for CB4.1 (Figure 5a), and maximum coefficients are shown for each organic class irrespective of the time at which they occur (Figure 5b). After formaldehyde itself, the ethylene and propene classes are the most reactive in terms of formaldehyde production. The sensitivity coefficients for CB4.1 are generally slightly higher than those for CB4. The three mechanisms show fairly close agreement for the maximum sensitivities to ethylene and acetaldehyde. As with ozone, the sensitivity of formaldehyde to propene is higher with CB4 and CB4.1 than with LCC.

Finally, Figure 6 shows instantaneous sensitivity coefficients for hydrogen peroxide, for the 12:1 case, in which final H_2O_2 concentrations ranged from 0.001 54 ppm with CB4 to 0.002 70 ppm with LCC. The sensitivity coefficients for H_2O_2 are shown for the end of the simulations, the time of both the peak H_2O_2 concentrations and the maximum sensitivities. For H_2O_2, sensitivity coefficients were uniformly higher for CB4.1 than for CB4, corresponding to higher H_2O_2 production with CB4.1. H_2O_2

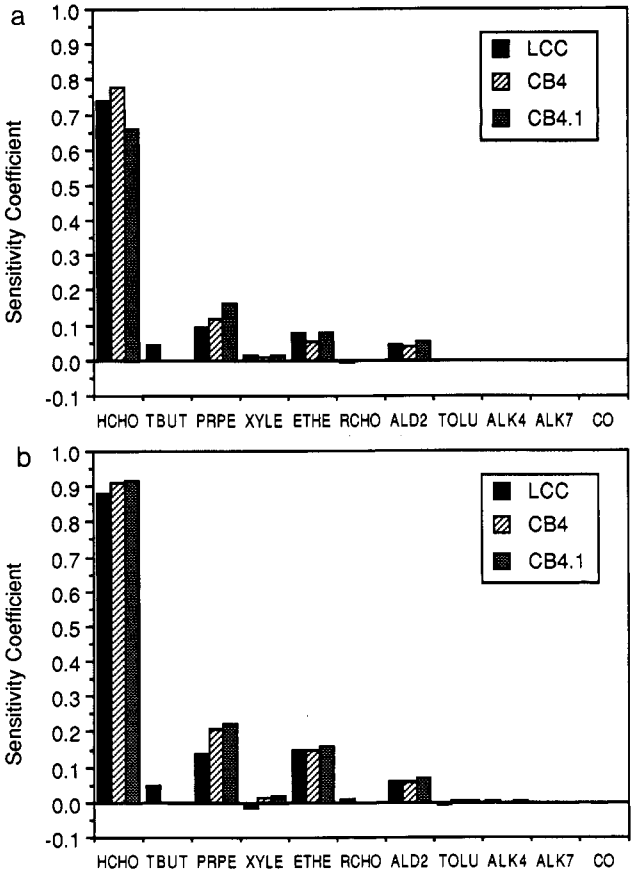

Figure 5. (a) Sensitivity of peak formaldehyde to the initial concentrations for each ROG class and (b) maximum sensitivity of formaldehyde to initial concentrations for case A (initial ROG:NO_x = 12:1). Sensitivity coefficients are given in units of ppm HCHO per ppm C.

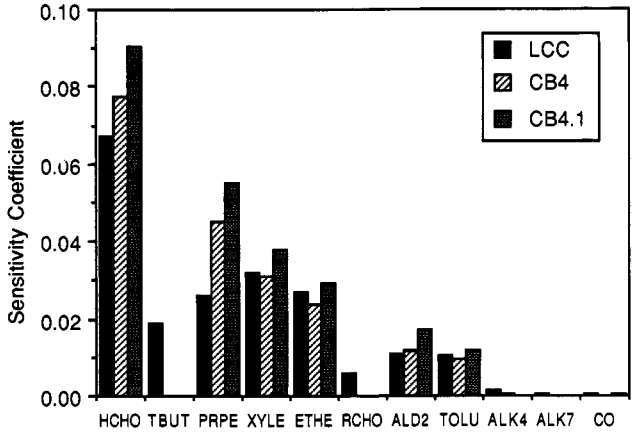

Figure 6. Sensitivity of peak hydrogen peroxide to the initial concentration for each ROG class for case A (initial ROG:NO_x = 12:1). Sensitivity coefficients are given in units of ppm H_2O_2 per ppm C.

sensitivity coefficients were also higher for CB4.1 than for LCC, for all species except for CO and the alkanes. Sensitivity coefficients for CB4 were higher than those of LCC for propene, formaldehyde, and acetaldehyde.

Given the few modifications made to CB4 to derive CB4.1, a straightforward way to understand how the differences affect the results of these two mechanisms is to conduct a few additional simulations, making the modifications one at a time. Thus, the first diagnostic test performed (test 1) was to add reaction 82 to CB4 but to retain the original rate expressions for reactions 46–48 (see Table II). Test 2 changed the rate expressions but left out reaction 82. The results of these tests are shown in Table VII, for comparison with the original results shown in Table VI. Adding reaction 82 (test 1) has little effect, with the exception of the final H_2O_2 concentration in case C. In this case the H_2O_2 concentration is significantly reduced and thus matches more closely the concentrations produced with CB4.1 and LCC.

Table VII. Predicted Concentrations (ppm) of Key Species after 12 h

		ROG/NO_x		
species	test case	12:1	6:1	24:1
O_3	CB4 test 1	0.333	0.111	0.232
	CB4 test 2	0.376	0.124	0.252
	LCC test 3	0.358	0.132	0.267
HNO_3	CB4 test 1	0.0654	0.0452	0.0265
	CB4 test 2	0.0703	0.0483	0.0284
	LCC test 3	0.0696	0.0579	0.0260
H_2O_2	CB4 test 1	0.00136	2.8×10^{-6}	0.0152
	CB4 test 2	0.00314	4.0×10^{-6}	0.0276
	LCC test 3	0.00303	6.6×10^{-6}	0.0151
HCHO	CB4 test 1	0.0399	0.0232	0.0451
	CB4 test 2	0.0423	0.0244	0.0480
	LCC test 3	0.0385	0.0220	0.0425
PAN	CB4 test 1	0.0483	0.0075	0.0284
	CB4 test 2	0.0459	0.00616	0.0249
	LCC test 3	0.0459	0.00873	0.0279

Concentrations of ozone and formaldehyde are affected more by the changes made to the rates of reactions 46–48 than by the addition of reaction 82. In particular, compared to the rates used in CB4, the rates used at 298 K in CB4.1 and test 2 tend to favor reaction 46 over reaction 47, and thus increase O_3 and HCHO concentrations. The result of altering the rates for reactions 46–48 could have been anticipated by examining the sensitivity results for CB4. For LCC, CB4, and CB4.1, Table VIII shows the reactions with the rate constants to which ozone has the highest sensitivity in case A. The table also shows the sensitivity of the ozone concentration to each rate constant, evaluated at the end of the simulation. Seminormalized sensitivity coefficients

$$s_{ij}' = p_j(\partial y_i/\partial p_j)$$

(in ppm) are shown, where p_j represents the rate constant of reaction j. CB4 reactions 46–48 are included in the top eight. Assuming that the changes in the rate constants are small enough for the combined response to them to be linear, the expected response is a 0.05 ppm increase in peak ozone over the concentration produced with the original CB4 mechanism. The results for test 2 show that the simulated response is a 0.04 ppm increase.

As in the comparison of CB4.1 with CB4, the relative rates of the acetyl peroxy radical + NO reaction versus the PAN formation reaction in CB4.1 are more favorable to O_3 and HCHO production than the relative rates of these reactions in LCC. The newly updated rates used in CB4.1 are in better agreement with recent studies (*26*, *27*) than those used in LCC. Acetyl peroxy radicals are produced via the reactions of acetaldehyde + OH and propene + OH, suggesting that the acetyl peroxy radical + NO_x reaction rates partially account for the enhanced reactivity of the acetaldehyde and propene classes in CB4.1 compared to LCC. In addition, the acetaldehyde photolysis rate used in CB4.1 and CB4 is higher than that used in LCC.

Coefficients for the sensitivity of formaldehyde to reaction rate constants in the 24:1 case identify a major reason for the discrepancy between the formaldehyde concentrations predicted with LCC versus those predicted with CB4.1. Table IX shows the reactions with the rate constants to which formaldehyde has the highest sensitivity in case C. Reactions involving the acetyl peroxy

Table VIII. Sensitivity of Peak Ozone to Reaction Rate Constants in Case A (12:1)

reaction	rxn no.	rate constant at 298 K, ppm^{-n} min^{-1} [a]	sensitivity coeff, ppm O_3
LCC Mechanism			
$NO_2 + h\nu \rightarrow NO + O$	(1)	0.3	0.144
$NO + O_3 \rightarrow NO_2 + O_2$	(5)	0.268×10^2	−0.133
$NO_2 + OH \rightarrow HNO_3$	(22)	0.168×10^5	−0.0943
$MCO_3 + NO_2 \rightarrow PAN$	(55)	0.757×10^4	−0.0745
$MCO_3 + NO \rightarrow HCHO + NO_2 + RO_2R + RO_2$	(54)	0.114×10^5	0.0742
$PAN \rightarrow MCO_3 + NO_2 + RCO_3$	(59)	0.221×10^{-1}	0.0647
$HCHO + h\nu \rightarrow 2HO_2 + CO$	(46)	0.677×10^{-3}	0.0634
$NO + HO_2 \rightarrow NO_2 + OH$	(26)	0.122×10^5	0.0249
CB4 Mechanism			
$NO_2 + h\nu \rightarrow NO + O$	(1)	0.3	0.143
$NO + O_3 \rightarrow NO_2 + O_2$	(3)	0.267×10^2	−0.133
$HCHO + h\nu \rightarrow 2HO_2 + CO$	(38)	0.677×10^{-3}	0.118
$NO_2 + OH \rightarrow HNO_3$	(26)	0.168×10^5	−0.115
$C_2O_3 + NO_2 \rightarrow PAN$	(47)	0.121×10^5	−0.0981
$C_2O_3 + NO \rightarrow HCHO + NO_2 + HO_2 + XO_2$	(46)	0.183×10^5	0.0977
$PAN \rightarrow C_2O_3 + NO_2$	(48)	0.228×10^{-1}	0.0847
$XYLE + OH \rightarrow 0.7HO_2 + 0.5XO_2 + 0.2CRES + 0.8MGLY + 0.3TO_2 + 1.1PAR$	(72)	0.362×10^5	0.0534
CB4.1 Mechanism			
$NO_2 + h\nu \rightarrow NO + O$	(1)	0.3	0.156
$NO + O_3 \rightarrow NO_2 + O_2$	(3)	0.267×10^2	−0.143
$NO_2 + OH \rightarrow HNO_3$	(26)	0.168×10^5	−0.116
$C_2O_3 + NO_2 \rightarrow PAN$	(47)	0.137×10^5	−0.0937
$C_2O_3 + NO \rightarrow HCHO + NO_2 + HO_2 + XO_2$	(46)	0.282×10^5	0.0932
$HCHO + h\nu \rightarrow 2HO_2 + CO$	(38)	0.677×10^{-3}	0.0887
$PAN \rightarrow C_2O_3 + NO_2$	(48)	0.260×10^{-1}	0.0832
$XYLE + OH \rightarrow 0.7HO_2 + 0.5XO_2 + 0.2CRES + 0.8MGLY + 0.3TO_2 + 1.1PAR$	(72)	0.362×10^5	0.0419

[a] The units of the rate constants depend on the order of the reactions.

Table IX. Sensitivity of Final HCHO to Reaction Rate Constants in Case C (24:1)

reaction	rxn no.	rate constant at 298 K, ppm^{-n} min^{-1} [a]	sensitivity coeff, ppm HCHO
LCC Mechanism			
$HCHO + h\nu \rightarrow CO$	(47)	0.133×10^{-2}	−0.0145
$HCHO + h\nu \rightarrow 2HO_2 + CO$	(46)	0.677×10^{-3}	−0.00888
$HCHO + HO_2 \rightarrow RO_2R + RO_2$	(50)	0.148×10^2	−0.00760
$HCHO + OH \rightarrow HO_2 + CO$	(48)	0.133×10^5	−0.00703
$NO_2 + h\nu \rightarrow NO + O$	(1)	0.3	0.00538
$PAN \rightarrow MCO_3 + NO_2 + RCO_3$	(59)	0.221×10^{-1}	0.00519
$ALD2 + OH \rightarrow MCO_3 + RCO_3$	(51)	0.236×10^5	0.00477
$MCO_3 + NO_2 \rightarrow PAN$	(55)	0.757×10^4	−0.00458
CB4.1 Mechanism			
$HCHO + h\nu \rightarrow CO$	(39)	0.133×10^{-2}	−0.0232
$HCHO + OH \rightarrow HO_2 + CO$	(37)	0.150×10^5	−0.0131
$HCHO + h\nu \rightarrow 2HO_2 + CO$	(38)	0.677×10^{-3}	−0.00984
$ALD2 + OH \rightarrow C_2O_3$	(43)	0.240×10^5	0.00793
$NO_2 + h\nu \rightarrow NO + O$	(1)	0.3	0.00745
$C_2O_3 + NO_2 \rightarrow PAN$	(47)	0.137×10^5	−0.00665
$PAN \rightarrow C_2O_3 + NO_2$	(48)	0.260×10^{-1}	0.00702
$NO + O_3 \rightarrow NO_2 + O_2$	(3)	0.267×10^2	−0.00526

[a] The units of the rate constants depend on the order of the reactions.

radical are clearly important. For LCC, however, the third-ranked reaction is that of $HCHO + HO_2$, which is not included in the CB4 mechanism. Recent evaluation of this reaction indicates that the LCC mechanism is in error (*31*). Reaction 50 is largely ineffective because the peroxy radical produced rapidly decomposes back into the reactants. Because the back-decomposition reaction was not included in LCC, a spurious effect was introduced. The results of omitting reaction 50 from LCC are shown as test 3 in Table VII. The change has marked effects on H_2O_2 and HCHO concentrations in cases A and C, resulting in closer agreement between CB4.1 and LCC.

To summarize, ozone concentrations predicted with CB4, CB4.1, and LCC showed close agreement, but larger disparity occurred for hydrogen peroxide and formaldehyde concentrations. Moreover, some discrepancies were noted in the sensitivity coefficients of individual organic classes in the three mechanisms. In particular, the reactivities of the alkanes and toluene classes in LCC tend to be high relative to the reactivities of the respective classes in CB4 and CB4.1; and the reactivities of the aldehydes and propene classes in CB4 and CB4.1 tend to be higher than those in LCC. Overall, for the cases simulated, the $HCHO + HO_2$ reaction in LCC and the revised acetyl peroxy radical reaction rates in CB4.1 appear to contribute most significantly to the differences in the predictions of the CB4, CB4.1, and LCC mechanisms. However, for initial ROG mixtures that are especially rich in alkanes or toluene, the differences between the LCC and CB4/CB4.1 mechanisms in the reactivities of these classes will also be important.

5. *Discussion*

The sensitivity coefficients shown in Figure 4 are consistent in both magnitude and ranking among classes with the incremental reactivities calculated by Carter and Atkinson (*12*) for similar cases, despite the use in the present study of simplifying assumptions such as constant photolysis rates. Carter and Atkinson also found HCHO, alkenes, and xylene to be the most reactive species in terms of ozone production and noted negative reactivities for toluene, xylene, and acetaldehyde in some cases. It is also notable that Carter's (*32*) maximum incremental reactivities and Russell et al.'s (*33*) reactivities usually fall within the range of sensitivities determined in this study for ROG to NO_x ratios of 6:1 and 12:1. The results of the DDM analysis also underscore Carter and Atkinson's conclusion that absolute reactivities are extremely sensitive to initial ROG to NO_x ratios and the duration of the simulations. In addition to these factors, this study shows that differences between mechanisms can also lead to significant differences in estimates of organic reactivities, even if the mechanisms show close agreement for predicted ozone concentrations.

When the differences between the organic reactivities predicted with LCC, CB4, and CB4.1 are highlighted, the results of this analysis have important implications for current discussions concerning regulatory use of organic reactivity scales for comparing emissions from variously fueled vehicles, including alternative fuels and reformulated gasoline. First, sensitivities of ozone to the same compounds in CB4 and CB4.1 differed by 10–20% in some cases. Thus for reactivity calculations, the modifications to CB4 that were recommended by Gery (*16*) appear to be important. Second, the sensitivities given by LCC and CB4.1 were often within about 20%, but in certain cases they differed by over a factor of 2. Of special significance with respect to motor vehicles, the sensitivities to the toluene classes in the two mechanisms differed substantially. Because toluene is a major component of automobile

exhaust, this suggests that airshed model-based calculations of the reactivity of automobile exhaust may differ depending on which mechanism is used.

The direct decoupled method offers two key advantages over previous approaches used to estimate incremental reactivities. First, earlier modeling studies and experimental investigations have been constrained to approaching the limit in eq 1 using changes in initial concentrations or modeled emissions on the order of a few percent (*10–12*). In contrast, the sensitivity coefficients calculated with the direct decoupled method are evaluated at the limit as the change in the parameter value approaches zero. Second, previous investigators have had to estimate reactivities for each compound class one class at a time, with some studies using hundreds of simulations (*32*), whereas with the DDM the sensitivity of all of the output species to all of the input species and reaction rates can be calculated simultaneously.

Comparing the results of this study with previous studies undertaken to compare CB4 and LCC illustrates additional advantages of the formal sensitivity analysis approach taken here. In earlier comparisons of CB4 and LCC, Dodge (*4*, *18*) used hundreds of simulations, including a variety of mixtures of organics and a range of temperatures, to explore the differences between the mechanisms. Clearly, additional simulations would have been needed in this study to examine the temperature dependence of CB4 and LCC predictions. Otherwise, the conclusions of the comparisons made by using the DDM generally support and in some instances elaborate upon Dodge's findings. A good example of the utility of the formal sensitivity analysis is the fact that it highlighted the HCHO + HO_2 reaction as a key discrepancy between CB4/CB4.1 and LCC. This difference was overlooked in the earlier comparisons of the two mechanisms (*4*, *18*).

Overall, Dodge (*18*) found good agreement for formaldehyde and ozone production with CB4 and LCC when typical urban mixtures of organics were studied. However, differences were noted when isolated organic compounds were used as inputs instead of a mixture. These conclusions are supported by the DDM analysis. For H_2O_2 concentrations, Dodge (*4*) found that agreement between CB4 and LCC at high ROG to NO_x ratios was significantly improved when the HO_2 + XO_2 reaction was added to CB4. Even with this reaction and at a 9:1 ROG to NO_x ratio, Dodge (*18*) found higher H_2O_2 yields with CB4 than with LCC for simulations in which propene and acetaldehyde were studied individually. The results of the current analysis are also consistent with these findings for H_2O_2.

Of the individual organic compound classes, the aromatics are of special note because the chemistry of the aromatics is considered highly uncertain. Dodge found that the toluene class in LCC was more reactive than that in CB4. The sensitivity analysis supports this finding for toluene. Also consistent with Dodge's results (*18*), but in contrast to previous findings of discrepancies between mechanisms in xylene chemistry, the sensitivities of O_3, HCHO, and H_2O_2 to the initial xylene concentrations in CB4.1 and LCC calculated in this study show fairly good agreement.

One case in which the DDM results do not agree with those of Dodge highlights the fact that the comparative performance of alternative mechanisms can depend on the ROG composition used. Dodge (*18*) found that CB4 gave relatively high formaldehyde and ozone concentrations in a simulation with a 9:1 ROG to NO_x ratio in which *trans*-2-butene was studied alone. This discrepancy was attributed to the use of acetaldehyde to represent *trans*-2-butene in CB4. In contrast to Dodge's results, application of the DDM indicated that ozone and formaldehyde sensitivities to acetaldehyde in CB4 and CB4.1 were similar to or lower than the sensitivities to *trans*-2-butene in LCC.

6. Conclusions

The results of this study generally support the conclusions of earlier comparisons of CB4 and LCC. However, the formal sensitivity analysis method brought out important characteristics of their comparative behavior that were not apparent in previous studies. And, because it calculates sensitivity coefficients for all species and rate parameters simultaneously, a single DDM application can replace numerous kinetic simulations performed in informal sensitivity analysis. The direct decoupled method thus provides a highly efficient tool for comparing competing mechanisms. Kinetic simulation results can be used to compare the predictions of different mechanisms but are difficult to interpret in terms of what gives rise to disagreements. Detailed examination of mechanism listings is useful for identifying potential sources of disagreement, but less helpful in determining which are the key discrepancies. The sensitivity analysis method thus fills a critical gap by providing a means of determining which discrepancies are most significant. Because chemical mechanisms developed for use in air-quality models are frequently revised and often need to be reevaluated, the efficiency and guidance afforded by the DDM approach are major benefits.

For the conditions studied, which approximate those of a smog chamber with a multicomponent mixture of input organics, ozone concentrations predicted with CB4, CB4.1, and LCC showed close agreement, but larger disparity occurred for hydrogen peroxide and formaldehyde concentrations. Sensitivity analysis of the three mechanisms indicated that the reactivities of the alkanes and toluene classes in LCC tend to be high relative to the reactivities of the respective classes in CB4 and CB4.1; and the reactivities of the aldehydes and propene classes in CB4 and CB4.1 tend to be high compared to those in LCC. Furthermore, the sensitivity analysis indicates that the incorrect treatment of the HCHO + HO_2 reaction in LCC and the differences between the acetyl peroxy radical reaction rates of LCC, CB4 and CB4.1 are key factors contributing to the differences in the predictions. In particular, recommended changes (*16*) to the rates of the acetyl peroxy radical + NO and PAN formation and decomposition reactions, which were incorporated into CB4.1, contribute to the relatively high "reactivity" of acetaldehyde and propene in that mechanism.

The direct decoupled method is also well-suited to the problem of quantitatively ranking organic compounds by their relative contributions to the formation of ozone or other secondary pollutants of concern. Use of the direct decoupled method offers two key advantages over reactivity estimation approaches that have been used previously. Sensitivity coefficients calculated with the direct decoupled method are exact reactivities, in that they are evaluated at the limit as the change in the input concentration of the organic under study approaches zero. And, with the DDM the sensitivity of all of the output species to all of the input species can be calculated at once rather than one at a time. Direct decoupled method sensitivity results were consistent with previous calculations of incremental reactivities, indicating HCHO, alkenes, and xylene to be the most reactive species in terms of ozone production. Carter and Atkinson (*12*) have previously emphasized the dependence of reactivity estimates on

simulation conditions. The current study has also shown that even for mechanisms giving peak ozone concentrations in close agreement the underlying reactivities they show for specific classes of organics can differ substantially.

Acknowledgments

Computer time, facilities, and assistance were provided by the Pittsburgh Super Computing Center and Cray Research, Inc. We greatly appreciate comments given by Marcia Dodge and William Stockwell.

Registry No. O_3, 10028-15-6; NO_x, 11104-93-1; HCHO, 50-00-0; H_2O_2, 7722-84-1.

Literature Cited

(1) Dunker, A. M.; Kumar, S.; Berzins, P. H. *Atmos. Environ.* **1984**, *18*, 311–321.
(2) Shafer, T. B.; Seinfeld, J. H. *Atmos. Environ.* **1986**, *20*, 487–499.
(3) Hough, A. M. *J. Geophys. Res.* **1988**, *93*, 3789–3812.
(4) Dodge, M. C. *J. Geophys. Res.* **1989**, *94*, 5121–5136.
(5) Dunker, A. M. *J. Chem. Phys.* **1984**, *81*, 2385–2393.
(6) McCroskey, P. S.; McRae, G. J. *Documentation for the Direct Decoupled Sensitivity Analysis Method—DDM*; Department of Chemical Engineering Report, Carnegie Mellon University: Pittsburgh, PA, 1987.
(7) Falls, A. H.; McRae, G. J.; Seinfeld, J. H. *Int. J. Chem. Kin.* **1979**, *11*, 1137–1162.
(8) Stockwell, W. R. Presented at XVII Informal Conference on Photochemistry, University of Colorado, Boulder, CO, June 1986.
(9) *Low-Emission Vehicles/Clean Fuels—Technical Support Document*; California Air Resources Board: Sacramento, CA, 1990.
(10) Dodge, M. C. *Atmos. Environ.* **1984**, *18*, 1657–1665.
(11) Carter, W. P. L.; Atkinson, R. *Environ. Sci. Technol.* **1987**, *21*, 670–679.
(12) Carter, W. P. L.; Atkinson, R. *Environ. Sci. Technol.* **1989**, *23*, 864–880.
(13) Gery, M. W.; Whitten, G. Z.; Killus, J. P. *Development and Testing of the CBM-IV for Urban and Regional Modeling*; EPA/600/3-88/012; U.S. Environmental Protection Agency: Research Triangle Park, NC, 1988.
(14) Gery, M. W.; Whitten, G. Z.; Killus, J. P. Dodge, M. C. *J. Geophys. Res.* **1989**, *94*, 12925–12956.
(15) Lurmann, F. W.; Carter, W. P. L.; Coyner, L. A. *A Surrogate Species Chemical Reaction Mechanism for Urban-Scale Air Quality Simulation Models*; EPA/600/3-87-014; U.S. Environmental Protection Agency: Research Triangle Park, NC, 1987.
(16) Gery, M. W. Atmospheric Research Associates, Inc., personal communication to Marcia Dodge, Nov 1990.
(17) Dodge, M. C. U.S. Environmental Protection Agency, personal communication, Mar 1991.
(18) Dodge, M. C. *J. Geophys. Res.* **1990**, *95*, 3635–3648.
(19) Carter, W. P. L.; Lurmann, F. W.; Atkinson, R.; Lloyd, A. C. *Development and Testing of a Surrogate Species Chemical Reaction Mechanism, Volumes 1 and 2*; EPA/600/3-86-031; U.S. Environmental Protection Agency: Research Triangle Park, NC, Aug 1986.
(20) Jeffries, H. E.; Sexton, K. G.; Salmi, C. N. *The Effects of Chemistry and Meteorology on Ozone Control Calculations Using Simple Trajectory Models and the EKMA Procedure*; EPA-450/4-81-034; U.S. Environmental Protection Agency: Research Triangle Park, NC, 1981.
(21) Leone, J. A.; Seinfeld, J. H. *Atmos. Environ.* **1985**, *19*, 437–464.
(22) Milford, J. B. Ph.D. Dissertation, Carnegie Mellon University, 1988.
(23) Carter, W. P. L.; Lurmann, F. W. *Evaluation of the RADM Gas-Phase Chemical Mechanism*; EPA/600/3-90/001; U.S. Environmental Protection Agency: Research Triangle Park, NC, 1990.
(24) Stockwell, W. R.; Lurmann, F. W. *Intercomparison of the ADOM and RADM Gas Phase Chemical Mechanisms*; Electric Power Research Institute: Palo Alto, CA, 1990.
(25) Bridier, I.; Caralp, F.; Loirat, H.; Lesclaux, R.; Veyret, B.; Becker, K. H.; Reimer, A.; Zabel, F. *J. Phys. Chem.* **1991**, *95*, 3594–3600.
(26) Tuazon, E. C.; Carter, W. P. L.; Atkinson, R. *J. Phys. Chem.* **1991**, *95*, 2434–2437.
(27) Kirchner, F.; Zabel, F.; Becker, K. H. *Ber. Bunsenges. Phys. Chem.* **1990**, *94*, 1379–1382.
(28) Grosjean, F.; Fung, K. *JAPCA* **1984**, *34*, 537–543.
(29) Baugues, K. *A Review of NMOC, NO_x and NMOC/NO_x Ratios Measured in 1984 and 1985*; EPA-450/4-86-015; U.S. Environmental Protection Agency: Research Triangle Park, NC, 1986.
(30) Gear, C. W. *Numerical Initial Value Problems in Ordinary Differential Equations*; Prentice-Hall: Englewood Cliffs, NJ, 1971; pp 209–228.
(31) Atkinson, R. *Atmos. Environ.* **1990**, *24A*, 1–41.
(32) Carter, W. P. L. *Development of Ozone Reactivity Scales for Volatile Organic Compounds*; Draft Final Report to the U.S. Environmental Protection Agency on Contract No. CR-814396-01-0; Statewide Air Pollution Research Center, University of California: Riverside, CA, Nov 1990.
(33) Russell, A. G.; McNair, L.; Odman, M. T. Airshed Calculation of the Sensitivity of Pollutant Formation to Organic Compound Classes and Oxygenates Associated with Alternative Fuels. *J. Air Waste Manage. Assoc.* **1992**, *42*, 174–178.

Received for review June 12, 1991. Revised manuscript received December 30, 1991. Accepted February 17, 1992. Early phases of this work were supported by the National Science Foundation under a Presidential Young Investigator Award CEE000659 to G.J.M. and by the PRECP program under Grant B-K5877-A-E from Battelle Pacific Northwest Laboratories.